CHEMISTRY
A EUROPEAN JOURNAL

DOI: 10.1002/chem.200600464

Synthesis of Novel Rod-Shaped and Star-Shaped Fluorescent Phosphane Oxides—Nonlinear Optical Properties and Photophysical Properties

Minh-Huong Ha-Thi,[a] Vincent Souchon,[a] Abdelwaheb Hamdi,[a] Rémi Métivier,[a] Valérie Alain,[a] Keitaro Nakatani,[a] Pascal G. Lacroix,[b] Jean-Pierre Genêt,[c] Véronique Michelet,*[c] and Isabelle Leray*[a]

Abstract: The design of a new class of fluorophores is presented. Some push–pull chromophores (D–π–A) containing polyphenylethynyl units and a phosphane oxide moiety were efficiently prepared from common intermediates. Straightforward syntheses gave novel one-armed, rod-shaped and three-armed, star-shaped fluorophores. The optical properties of the resulting star-shaped derivatives were evaluated, showed high fluorescence quantum yields, and their excitation induces very efficient charge redistribution. Moreover, thanks to their push–pull character, the molecules exhibited significant second-order NLO properties with good transparency, up to $67 \cdot 10^{-30}$ esu at 1907 nm, with an absorption λ_{max} at 369 nm. The effect of the donor group and of the number of phenylethynyl arms have been studied in this work.

Keywords: charge transfer · fluorescence spectroscopy · nonlinear optics · phosphane oxide · solvatochromism

Introduction

Over the past few years significant research has been directed toward the development of organic materials for potential application in molecular photonic devices[1] and the development of sensors.[2] Interest in these materials is primarily due to the infinite numbers of possible molecular structures with the desired properties, by virtue of the tremendous capabilities of organic synthesis.

For the development of a new fluorescent molecular sensor consisting of a recognition moiety linked to a fluorescent moiety, the choice of the fluorophore is of major importance. This component should convert the recognition event into an optical signal as the result of a change in its photophysical characteristics caused by the perturbation of various photoinduced processes (electron transfer, energy transfer, charge transfer) by the bound species.[3] A particular advantage of fluoroionophores based on cation control of photoinduced charge transfer is that the absorption and fluorescence spectra are shifted upon cation binding[4] so ratiometric measurements are possible: the ratio of the fluorescence intensities at two appropriate emission or excitation wavelengths provides a measure of the cation concentration independent of the probe concentration and insensitive to incident light intensity, scattering, inner filter effects, and photobleaching. To ensure better sensitivity, different photophysical properties of the fluorophore—such as high molar extinction coefficient, high fluorescence quantum yield, and good photostability—must be considered, which has prompted us to design new charge-transfer molecules. Among the existing fluorophores, poly(phenylene)ethynylenes and other arylethynyl fluorophores are very attractive because of their high photostability, their electron-transport abilities, and their intense fluorescence emissions.[5] A series of push–pull chromophores (D–π–A), each containing a polyphenylethynyl unit as a conjugated bridge, had already been

[a] M.-H. Ha-Thi, V. Souchon, Dr. A. Hamdi, Dr. R. Métivier, Dr. V. Alain, Prof. K. Nakatani, Dr. I. Leray
CNRS UMR 8531 Laboratoire de Photophysique et Photochimie Supramoléculaires et Macromoléculaires
Département de Chimie, ENS-Cachan
61 avenue du Président Wilson, 94235 Cachan Cedex (France)
Fax: (+33) 147-402-454
E-mail: icmleray@ppsm.ens-cachan.fr

[b] Dr. P. G. Lacroix
Laboratoire de Chimie de Coordination du CNRS
205 route de Narbonne, 31077 Toulouse (France)

[c] Prof. J.-P. Genêt, Dr. V. Michelet
Laboratoire de Synthèse Sélective Organique et Produits Naturels
E.N.S.C.P., UMR7573, 11 rue P. et M. Curie
75231 Paris Cedex 05 (France)
Fax: (+33) 144-071-062
E-mail: veronique-michelet@enscp.fr

Supporting information for this article is available on the WWW under http://www.chemeurj.org/ or from the author.

studied.[6] In these systems, photoexcitation induces substantial charge separation, as evidenced by the large solvatochromic shifts observed in their emission spectra, and it is possible to take advantage of the push–pull characters of these systems for nonlinear applications.[7]

In the course of our recent ongoing program directed towards the production of novel fluorophores, we have recently described the synthesis of two novel molecules **1a** and **2a** (Scheme 1), each bearing a phosphane oxide as an acceptor group and a methoxy group or groups as donor moieties.[8] These systems exhibit high fluorescence quantum yields, and their excitation induces very efficient charge redistribution in the molecules. In anticipation that the donor group might influence either the fluorescence or the nonlinear properties, an easy route to analogues of **1a** and **2a** was desired. Moreover, the influence of substitution of the star-shaped phosphane oxides may be evaluated through the preparation of two families bearing mono- or trisubstituted fluorescent arms. There being no precedent for and no data relating to such derivatives, we therefore wish to describe here our full study involving a series of fluorescent probes, including their synthesis, their photophysical and nonlinear optical properties, and molecular orbital calculations.

Results and Discussion

Synthesis: We turned our attention to the preparation of the dimethylamino derivatives **1b** and **2b** and the triaryl derivative **1c** (Scheme 1), as the NMe_2 group is known to be a stronger donor than the methoxy group. An anthracenyl adduct **3** was also targeted, this being particularly attractive from the point of view of its ability to absorb in the visible region.[9] We envisaged an easy route to such derivatives starting from the triarylphosphane oxides **1d**[8] or **2d**, which could be prepared from commercially available 4-bromophenylacetylene (**4**) (Scheme 2).

The triarylphosphane oxides **1a–c** were synthesized from **1d**[8] through Pd-catalyzed Sonogashira couplings

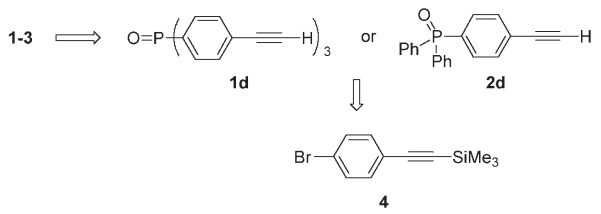

Scheme 2. Retrosynthesis for phosphane oxide fluorescent probes.

(Scheme 3). Phosphane oxide **1a** was prepared by the previously described procedures,[8] whilst the easy route to phosphane oxide **1b** was based on the synthesis of iodide **6**, starting from commercially available products **7** and **8**. The Sonogashira coupling was optimized in the presence of 9 mol% of $[Pd(PPh_3)_4]$ and afforded the desired phosphane oxide in 70% isolated yield. The known 4-iodo-*N*,*N*-dimethylaniline (**9**)[10] could also be treated with triarylphosphane **1d** to provide the desired product **1c** efficiently in 74% yield. We therefore had a route to three star-shaped triarylphosphane oxides in good overall yields and in a straightforward synthesis.

Aiming to examine the influence of mono- and trisubstituted fluorescent arms, we also envisaged the preparation of the monosubstituted arylphosphane oxides **2a** and **2b** (Scheme 4). Phosphorylation with the Grignard reagent derived from the commercially available 1-(4-bromophenyl)-2-(trimethylsilyl)acetylene (**4**) in the presence of chlorodiphenylphosphane was followed by phosphorus oxidation and desilylation reaction, this high-yielding, three-step process giving the desired adduct **2d** in 47% overall yield. We,[8] and others,[11] have previously reported alternative strategies starting from chlorodiphenylphosphane and diphenylphosphane, respectively, but these both afforded the diphenylarylethynylphosphane in lower isolated yields. The Sonogashira couplings of the phosphane oxide **2d** were carried out either with iodo derivatives **5** and **6** or with the known bromonaphthyl **10**,[9] the corresponding substituted phosphane

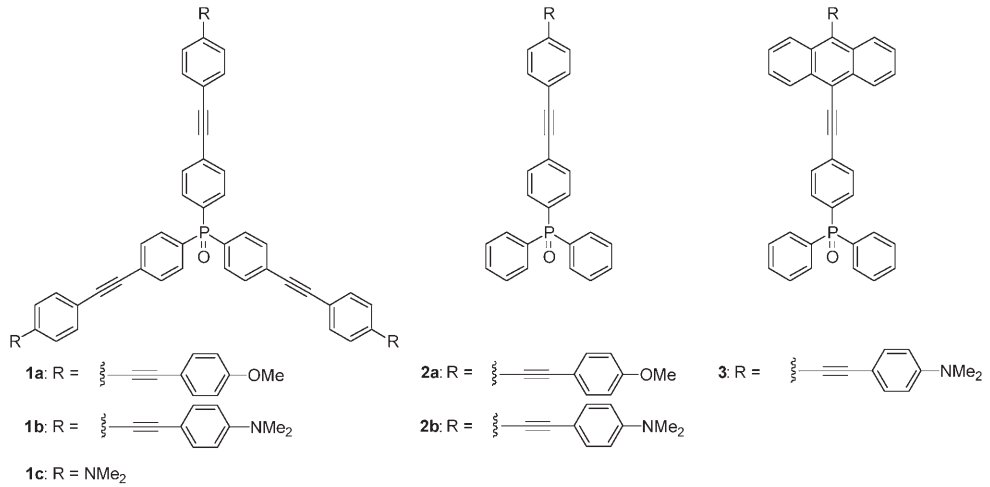

Scheme 1. Phosphane oxide fluorescent probes.

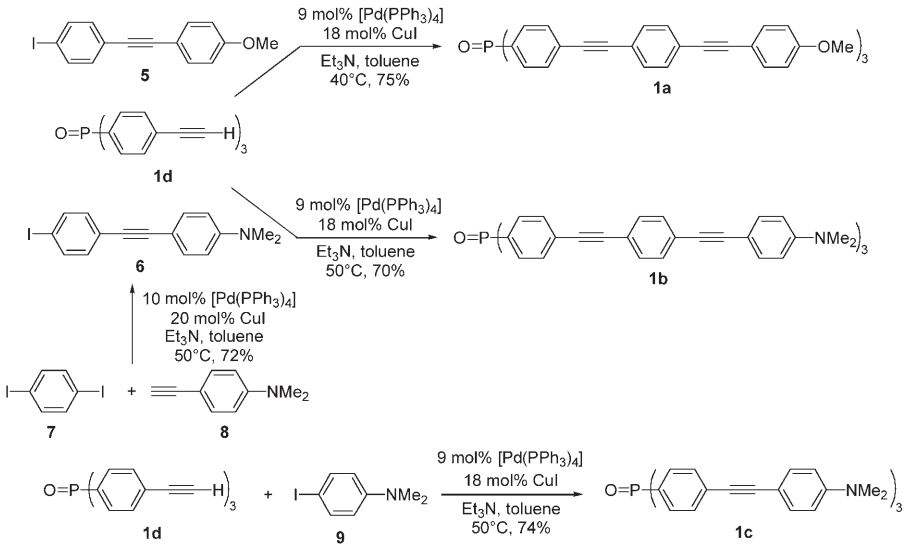

Scheme 3. Synthesis of triarylphosphane oxides.

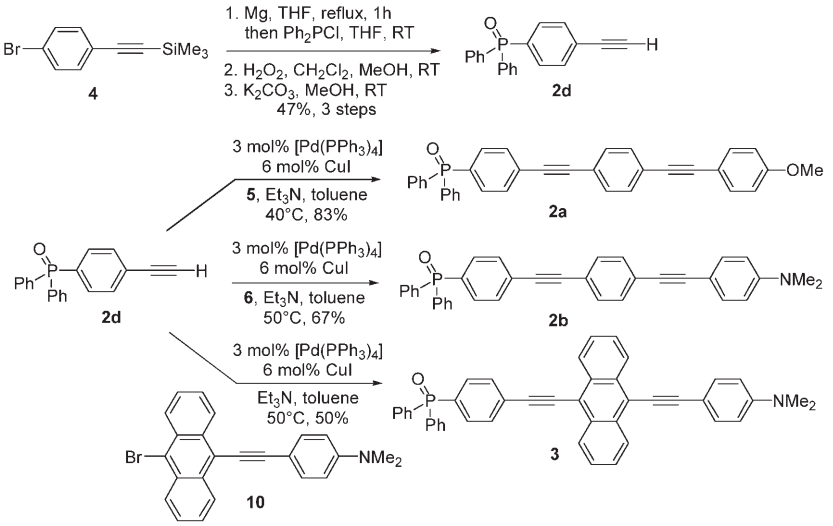

Scheme 4.

oxides **2a**, **2b**, and **3** being isolated in moderate to good yields (50–83%).

Having prepared the one-armed, rod-shaped and three-armed, star-shaped fluorescent probes, we next turned our attention to the photophysical properties of these novel derivatives.

Photophysical properties: The photophysical properties of the related phosphane oxide derivatives are given in Table 1, whilst the absorption and emission spectra of monosubstituted and star-shaped phosphane oxides are given in Figure 1a and b, respectively. Time-resolved fluorescence measurements were performed by the single-photon counting method with picosecond laser excitation; the fluorescence decays for the different phosphane oxides are shown in Figure 2. Satisfactory fits can be obtained by considering a single exponential ($\chi_R^2 < 1.25$). The radiative and nonradiative rate constants are related to the corresponding emission quantum yield and lifetime by $k_r = \Phi/\tau$ and $k_{nr} = (1-\Phi)/\tau$ (Table 1).

The fluorophores containing phenylethynyl bridges (**1** and **2**) each show good transparency in the visible region and an intense absorption band in the near UV/blue visible range, which can be attributed to an intramolecular charge transfer (ICT) upon $S_0 \rightarrow S_1$ excitation.[11] The tolane skeleton presents the advantage of avoiding the chemically and photochemically readily induced *cis*/*trans* isomerizations that can occur in the corresponding stilbenes, whilst the acetylenic triple bonds also induce hypsochromic shifts relative to the corresponding chromophores containing double bonds, producing an enhancement of the transparency range, a highly desirable property when NLO properties are considered. The absorption maxima depend both on the natures of the peripheral

Table 1. Photophysical properties of the phosphane oxide derivatives in chloroform. Maxima of one-photon absorption λ_{abs} [nm] and of steady-state emission λ_{em} [nm], molar absorption coefficient ε [10^4 M^{-1}cm^{-1}], fluorescence quantum yield Φ_F, fluorescence lifetime τ [ns], radiative k_r [10^8 s^{-1}] and nonradiative rate k_{nr} [10^8 s^{-1}] constants, together with computed optical data (absorption maxima λ_{max} [nm], and oscillator strength *f*).

Product	λ_{abs} [nm]	ε [10^4 M^{-1}cm^{-1}]	*f*	λ_{em} [nm]	Φ_F[b]	τ [ns]	k_r [10^8 s^{-1}]	k_{nr} [10^8 s^{-1}]	λ_{max}[d][nm]	*f*[c,d]
1a	338	17.7	4.06	392	0.77	0.74	10.41	3.11	315	6.1
1b	369	12.5	2.29	478	0.56	1.52	3.68	2.89	317	6.1
1c	367	6.5	1.49	428	0.58	1.88	3.09	2.23	294	4.1
2a	335	5.9	1.42	388	0.76	0.78	9.74	3.08	312	2.4
2b	369	4.1	0.86	471	0.66	1.52	4.34	2.24	319	2.4
2c	481	3.1	0.61	573	0.78	2.81	2.78	0.78	418	1.43

[a] The detailed HOMO–LUMO transitions and the various compositions of CI expansion are reported in the Supporting Information. [b] Fluorescence quantum yield with a 10% random error. [c] Computed optical data. [d] Overestimated value.

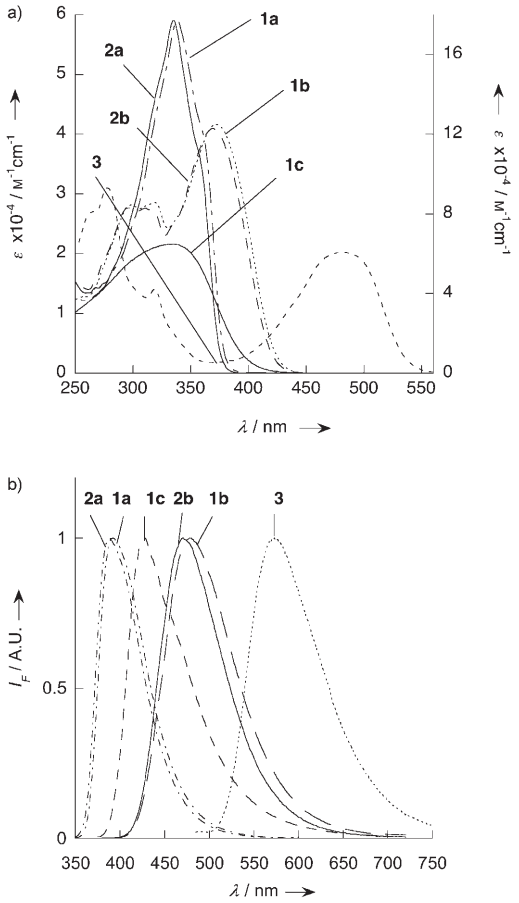

Figure 1. a) Absorption of phosphane oxide derivatives in chloroform (left ordinate: rod-shaped phosphane oxides **2a**, **2b**, and **3**; right ordinate: star-shaped phosphane oxides **1a** and **1b**). b) Corrected normalized emission spectra of phosphane oxide derivative in chloroform.

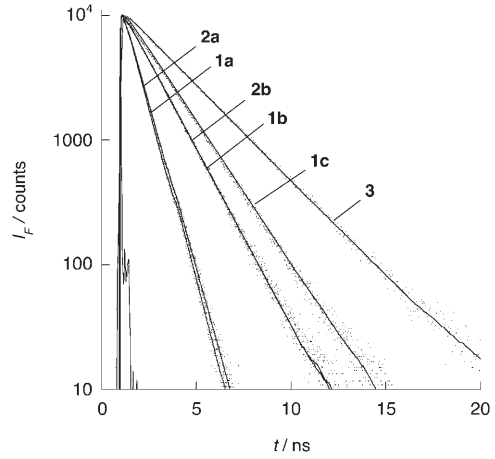

Figure 2. Fluorescence decays of phosphane oxide derivatives in chloroform.

substituents and on the lengths of the conjugated arms. As would be expected, bathochromic shifts are observed with increasing electron density of the donating groups ($OCH_3 <$ $N(CH_3)_2$). Furthermore, it was shown that red shifting in the absorption band is observed with increasing conjugation length (**1c** compared with **1b**) due to an extension of the π-conjugation. In the case of the anthracenyl-based fluorophore, the absorption is shifted by about 100 nm, an effect interpreted in terms of better π-orbital delocalization due to the presence of the anthracenyl bridge. All of these molecules are strongly fluorescent in chloroform, with fluorescence quantum yields ranging from 0.55 to 0.78. The value of the quantum yield and the radiative rate constant are similar to those reported for the strongly emitting fluorophores based on rod-shaped oligo(π-phenyleneethynylenes).[12] As also observed in the absorption, bathochromic shifting of the emission spectra in chloroform is observed with increasing donating group power (λ_{em} for **1a** = 388 and λ_{em} for **1b** = 471 nm). This effect is more pronounced for the emission than for the absorption, suggesting an enhancement of the dipole moment in the excited state. The shape, molar absorption coefficient (normalized to the same number of fluorophores), fluorescence quantum yield, and fluorescence lifetime are similar for compounds **1a** and **2a**, indicating weak interaction between the fluorophores; the same tendency has been observed for compounds **1b** and **2b**. Thus, from these experimental data, it can be considered that the emitting states in the star-shaped fluorophores **1a** and **1b** are located on single branches of the fluorophores. Similar effects have previously been observed in the case of multibranching dipolar chromophores.[13] The emission efficiencies (Φ_F, k_r) correlate with the electron-donating abilities of the donor groups and the π-extensions, the k_r values being found to be about three times higher for **1a** than for **1b** and for **2a** than for **2b**.

These experimental features can be interpreted further by use of semiempirical procedures at the intermediate neglect of differential overlap (INDO) level; the experimentally obtained data are compared to the semiempirical (INDO) spectra in Table 1. Both experimentally measured and calculated spectra are dominated by intense and low-lying bands, with a tendency towards slight blue shifting (about 50 nm) on passing from experimentally measured to calculated values. Calculation indicates that the origins of these bands seem to be slightly different in the one-armed (**2a**, **2b**) and three-armed molecules (**1a**, **1b**). While single, HOMO–LUMO-based (1→2) electron transitions contribute to the intense bands in the one-armed chromophores, sets of two (1→2 and 1→3) transitions mixing excitations between six orbitals are involved in the description of the bands in three-armed systems (see Supporting Information for details on electron transition bands). This may be explained by the fact that C_3 symmetry axes were postulated for the three-armed molecules. The six orbitals involved in the charge-transfer transitions of the three-armed derivatives are therefore reminiscent of the HOMOs and LUMOs of the one-armed parent molecules, and finally the overall physical properties are equivalent in any case. Thus, apart from these differences between experimentally measured and calculated data, there is satisfactory correlation between the theory-

derived values and the data relating to UV/Vis absorption maxima and oscillator strength of the transition (Table 1). The observation that the presence of a better electron donor (dimethylamino) lowers the energies of the transitions strongly supports a push–pull character in these systems, and hence the potential for sizeable quadratic molecular hyperpolarizabilities (β) in these molecules, as discussed in the next section. HOMO and LUMO orbitals for **2a** and **2b** are shown in Figure 3a and b. In each case a charge transfer from the R-C_6H_4-C≡C- and the -C≡C-$C_6H_4P(O)(C_6H_5)_2$ fragments is evident, with a tendency towards stronger effects in the case of the Me_2N-containing molecule, consistently with the more strongly electron-donating character of the amine.

Solvatochromism effects of the new fluorophores (**1b**, **1c**, **2b**, and **3**) were studied and compared with the previously observed phosphane oxide data[8] (Table 2). In contrast with the small bathochromic shifts observed in the absorption spectra, an important red shifting of the emission spectra was observed (Figure 4 for **2b**). The Stokes shift for **2b** in CH_3CN, for example, is 10521 cm^{-1}, indicating that the dipole moment of the phosphane oxide is much larger in the excited state than in the ground state.

According to the Lippert–Mataga equation,[14] the Stokes shift can be related to the difference in dipole moment between the ground and the excited states:

$$\nu_a - \nu_f = \frac{2}{hca^3}(\mu_e - \mu_g)^2 \Delta f + \text{constant} \quad (1)$$

where ν_a and ν_f are the frequencies of the absorption and

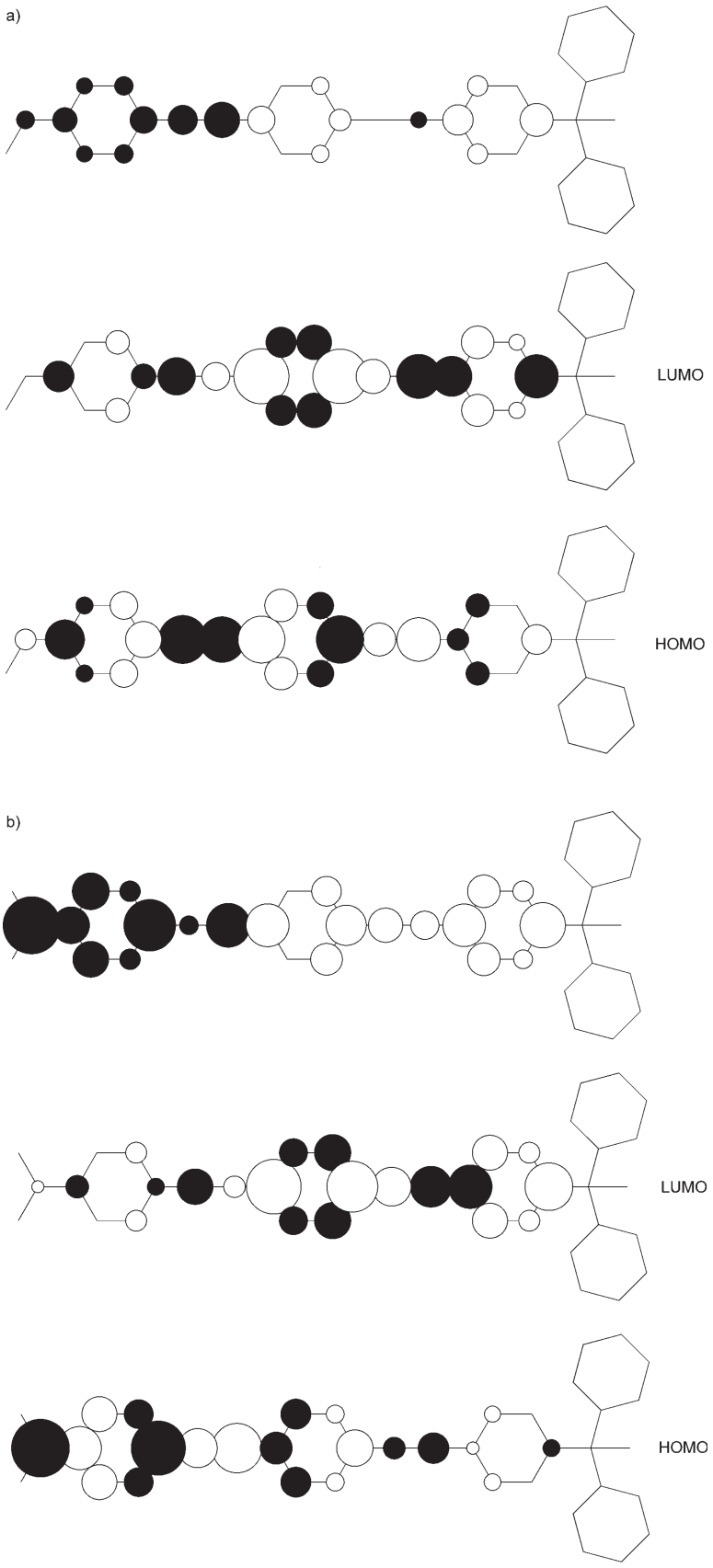

Figure 3. HOMOs (bottom) and LUMOs (middle) for **2a** (a) and **2b** (b) with the associated charge transfer (top). The white (black) contributions in the charge-transfer drawing correspond to increases (decreases) in the electron density upon excitation.

Table 2. Solvatochromism of **1a**, **1b**, **1c**, **2a**, **2b**, and **3**. λ_{abs} [nm], λ_{em} [nm], and Φ_F[a] as the function of the orientation polarizability Δf.

		Solvent						
		cyclohexane	dioxane	$CHCl_3$	CH_2Cl_2	DMSO	EtOH	CH_3CN
Product	Δf	−0.001	0.021	0.149	0.219	0.265	0.290	0.306
1a[b]	λ_{abs} [nm]	335	336	338	338	338	336	334
	λ_{em} [nm]	366	379	392	406	443	418	428
	Φ_F	0.78	0.89	0.77	0.73	0.71	0.86	0.79
1b	λ_{abs} [nm]	364	369	370	373	[c]	[c]	[c]
	λ_{em} [nm]	409	464	478	518	[c]	[c]	[c]
	Φ_F	[b]	0.56	0.57	0.63	[c]	[c]	[c]
1c	λ_{abs} [nm]	364	359	367	364	371	366	362
	λ_{em} [nm]	374	418	428	463	529	502	516
	Φ_F	0.46	0.43	0.58	0.44	0.06	0.07	0.04
2a[b]	λ_{abs} [nm]	333	333	335	334	336	333	331
	λ_{em} [nm]	364	374	388	402	434	412	422
	Φ_F	0.77	0.97	0.76	0.78	0.75	0.81	0.94
2b	λ_{abs} [nm]	363	367	369	370	377	367	367
	λ_{em} [nm]	399	459	471	511	615	579	600
	Φ_F	0.73	0.73	0.66	0.69	0.04	0.10	0.07
3	λ_{abs} [nm]	[b]	480	481	489	501	479	485
	λ_{em} [nm]	[b]	567	570	603	690	633	665
	Φ_F	[b]	0.60	0.78	0.51	0.03	0.48	0.08

[a] Fluorescence quantum yield with a 10% random error. [b] Data previously reported in ref. [8] [c] Not soluble.

er the slope and the higher the enhancement of the dipole moment in the excited state. Interestingly the slope is the same for compounds containing the same donor (comparison between **1a** and **2a** and between **1b** and **2b**). This can again be explained by the emitting excited states having the same nature in the case of the star-shaped molecule and in the case of the rod-shaped molecule. It should also be noted that the slopes for **1b** and **1c** are the same. In the case of **3** the slope is smaller, which can be explained in terms of a minor delocalization of the charge in the excited state due to the presence of the anthracenyl moiety.

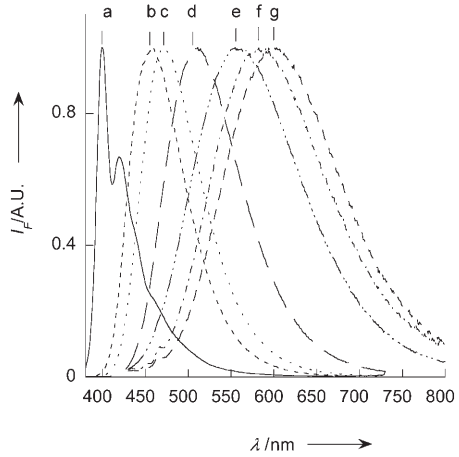

Figure 4. Corrected emission spectra of **2b** in different solvents. a) Cyclohexane. b) Dioxane. c) $CHCl_3$. d) CH_2Cl_2. e) EtOH. f) CH_3CN. g) DMSO.

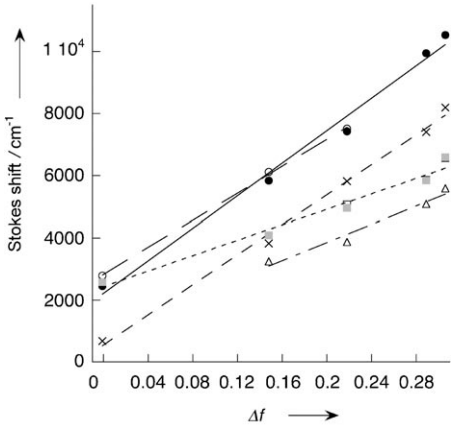

Figure 5. Lippert–Mataga correlations of fluorophores **1a** (●), **2a** (○), **1b** (×), **2b** (□), **2c** (■), and **3** (△).

fluorescence maxima, respectively, h is Planck's constant, c is the velocity of light, a is the radius of the cavity in which the solutes resides, and Δf is the orientation polarizability, defined as:

$$\Delta f = \frac{\varepsilon-1}{2\varepsilon+1}-\frac{n^2-1}{2n^2+1} \quad (2)$$

where ε is the static dielectric constant of the solvent and n is the optical refractive index of the solvent.

As shown in Figure 5, plots of the orientation polarizabilities (Δf) against the Stokes shifts in various solvents are linear for the different compounds. The slopes depend on the natures of the donors: the stronger the donor, the steep-

To determine the enhancements of the dipolar moments in the excited states, one key parameter was the determination of the Onsager cavities. In the case of an elongated molecule, overestimation of the radius cavity can often occur through the use of the distance between donor and acceptor, which gives rise to uncertainty in the determination of the enhancement of the dipole moment in the molecule, so the use of an ellipsoidal cavity model is more appropriate.[15] The $\Delta\mu$ values for **2a** and **2b** were also evaluated by INDO[16] and were found to be 10 D and 17 D, respectively: lower than, but in a satisfactory agreement with, the experimentally measured values (Table 3).

The solvent effects on fluorescence efficiency were then studied for compounds **2a** and **2b**. Table 4 displays the obtained fluorescence quantum yields, fluorescence lifetimes, and the corresponding radiative and nonradiative rate con-

Table 3. Experimentally measured dipole moments and hyperpolarizabilities (β in 10^{-30} esu) at 1907 nm for **1a**, **1b**, **1c**, **2a**, **2b**, and **3**.

Product	μ [D]	$\Delta\mu$ [D]	β [10^{-30} esu]	β_0 [10^{-30} esu]
1a	5.1	15	40	32
1b	7.1	20	67	54
1c	6	15	46	
2a	4.2	15	24	20
2b	4.8	22	51	43
3		12		

stants. Whilst the fluorescence quantum yield of **2a** did not change very much with increasing solvent polarity, a significant decrease in the fluorescence quantum yield with increasing solvent polarity was observed in the case of **2b**, and this result was accompanied by an enhancement of the nonradiative rate constant. Such an effect can be interpreted in terms of specific interaction between the amino nitrogen group of **2b** and the solvent in the excited state, as previously observed with similar compounds.[17]

Table 4. Photophysical properties of the phosphane oxides **2a** and **2b** in different solvents. Fluorescence quantum yields Φ_F, fluorescence lifetimes τ [ns], radiative k_r and nonradiative k_{nr} rate constants [10^8 s^{-1}].

	2a				**2b**			
Solvent	Φ_F	τ [ns]	k_r [10^8 s^{-1}]	k_{nr} [10^8 s^{-1}]	Φ_F	τ [ns]	k_r [10^8 s^{-1}]	k_{nr} [10^8 s^{-1}]
cyclohexane	0.77	0.63	12.22	3.65	0.76	0.87	8.74	2.76
dioxane	0.92	0.73	12.60	1.10	0.73	1.43	5.10	1.89
$CHCl_3$	0.76	0.78	9.74	3.08	0.66	1.52	4.34	2.24
CH_2Cl_2	0.78	0.87	8.97	2.53	0.69	2.12	3.25	1.46
DMSO	0.75	1.17	6.41	2.14	0.06	0.42	1.43	22.38
EtOH	0.81	1.03	7.86	1.84	0.18	0.76	2.37	10.79
CH_3CN	0.89	1.13	7.88	0.97	0.11	0.61	1.80	14.59

Nonlinear optical properties: Measurements of the molecular hyperpolarizabilities of the phosphane oxides were made, in order to investigate and thus illustrate potential optical applications.

Since EFISH gives the scalar product ($\mu\beta$) of the dipole moment by the hyperpolarizability, it was then possible to obtain the projection of β on the dipole moment direction (noted β for sake of simplicity) from independent measurement of μ. In both the one-armed and the three-armed series we had observed an increase in β through the replacement of methoxy groups by dimethylamino moieties (Table 3). As would be expected from the better electron-donating capacity of the latter group, the same tendency was observed for the μ value. Although compound **1c** has weaker β and μ values than its analogue **1b**, arising from a shorter conjugated chain between the push and pull moieties, it competes well with other push–pull diphenylacetylenes reported in the literature (e.g., 46×10^{-30} cm^5 esu^{-1} for 4,4′-dimethylaminonitrodiphenylacetylene[7b]), but is significantly smaller than that obtained for 1,3,5-triazine substituted with a dimethylaminophenylethynyl group.[18] Such an effect can be explained by the fact that the 1,3,5-triazine group is a better withdrawing group than the nitro or the phosphane oxide group. To the best of our knowledge, only powder tests of molecules possessing three phenyl rings and two acetylene functions have been reported.[7a] Multiplying the number of arms resulted in a slight increase in β, which will be discussed further.

NLO response in chromophores 2a and 2b: According to the simplified, but widely used "two-level" description of the NLO response, the hyperpolarizabilities of "push–pull" one-dimensional molecules (e.g., **2a** and **2b**) have their origin in intense low-lying transitions of energy E and oscillator strength f, involving a charge-transfer character between a ground (g) and an excited (e) state (dipole moment change $\Delta\mu = \mu_e - \mu_g$), according to the following relationship:[19,20]

$$\beta = \frac{3e^2\hbar f\Delta\mu}{2mE^3}\times\frac{E^4}{(E_2-(2\hbar\omega)^2)(E^2-(\hbar\omega)^2)} \quad (3)$$

in which $\hbar\omega$ is the energy of the incident laser beam. In the cases of compounds **2a** and **2b** the lowest energy transitions (1→2) are very intense (large f values) and can be assumed to be dominant in the description of the NLO properties. Furthermore, the data gathered in the Supporting Information indicate that each transition is based on the corresponding single HOMO→LUMO excitation, contributing at levels of 89 and 83% of the effect in **2a** and **2b**, respectively. Therefore, it can readily be assumed that the description of the charge transfer associated with the HOMO→LUMO excitation provides the rationale for understanding of the microscopic origin of the NLO response in these "push–pull" chromophores.

Experimentally measured and computed values also support the idea that the charge transfer (and hence the hyperpolarizability) is enhanced when the strength of the donating substituent is stronger. Within the approximation of the two-level description [Eq. (3)], the current set of $\Delta\mu$, f, and E parameters gives computational β values of 43 and 84×10^{-30} cm^5 esu^{-1} for **2a** and **2b**, respectively. These values are somewhat larger than the experimentally ascertained 24 and 51×10^{-30} cm^5 esu^{-1} values, but it is well known that the two-level description frequently gives an overestimation of molecular hyperpolarizabilities.[21]

NLO response in three-armed 1a and 1b and comparison with the one-armed analogues: Because of the presence of the phosphane oxide moieties the three arms are not coplanar, resulting in a dipolar (not octupolar) geometry. If a one-dimensional model along the C_3 symmetry axis is considered, the projection of the dipole moment change ($\Delta\mu$) associated with the two degenerate (1→2 and 1→3) transitions should be viewed as the resulting contribution to the NLO response. This approach gave hyperpolarizabilities

equal to 15 and 22×10^{-30} cm^5 esu^{-1} for **1a** and **1b**, respectively. As would be expected, these values are significantly lower than the experimentally measured (42 and 67×10^{-30} cm^5 esu^{-1}) data because they arise from an oversimplified picture in which $\beta = \beta_{zzz}$ and do not take into account the contribution of the β_{zxx} and β_{zyy} tensor components, which will probably be important in the current geometry. Unlike in the situation encountered in the simple "push–pull" **2a** and **2b** chromophores, this analysis therefore suggests that a model based on simple charge-transfer processes may not be fully reliable in these systems.

The ratios between the μ and β values of the three-armed star-shaped molecules and their one-armed analogues range between 1.2 and 1.7. Theoretically, the relationship between the two types of molecules should be:[22]

$$\mu_3 = 3\mu_1\cos\theta \quad (4)$$

$$\beta_3 = 3\beta_1\cos\theta \quad (5)$$

where the indices 1 and 3 refer to the one- and three-armed molecules, respectively, and θ to the angle between each arm and the C_3 axis. The terms μ_3 and β_3 are along the C_3 axis, whereas μ_1 and β_1 are along the molecule's main axis, and are the components involved in EFISH data.

In the calculated structures of the three-armed chromophores, each dipolar arm makes an angle of $\theta = 66°$ with the C_3 axis, so the above ratio would be 1.22. The experimentally obtained results are therefore consistent with the theory within the experimental errors of the EFISH measurements.

Conclusion

We have synthesized a series of new phenylethynyl phosphane oxides bearing different donor groups. To study various degrees of donor and acceptor strength, the influence of the substitution and the nature of the π-conjugation element were investigated through the preparation of six analogues. The geometries of these fluorophores were optimized, resulting in one-armed, rod-shaped and three-armed, star-shaped derivatives. The absorption and emission spectra revealed that the electronic properties of these fluorophores were strongly affected by the nature of the donor, the length, and the nature of the π-conjugation. The internal charge-transfer characters of the transitions were investigated by solvatochromism measurements and it was found that highly efficient charge redistribution occurred upon excitation both for the one-armed, rod-shaped fluorophores and for their three-armed, star-shaped counterparts. Estimations of the enhancements of the dipole moments in the excited states were performed, showing that enhancement is higher in cases of compounds bearing the more strongly electron-donating dimethylamino group. The photophysical properties of the star-shaped fluorophores and rod-shaped fluorophores were found to be the same, indicating that the emitting state in each star-shaped derivative is located on a single branch. Because of their strong push–pull characters, the chromophores exhibit sizeable NLO responses in solution, with a tendency towards larger hyperpolarizabilities in the three-armed series.

Experimental Section

General procedure: Reagents were commercially available from Acros, Aldrich, or Avocado and were used without further purification unless otherwise stated. Cyclohexane, dioxane, chloroform, dichloromethane, dimethylsulfoxide, and acetonitrile (Aldrich, spectrometric grade or SDS, spectrometric grade) were employed as solvents for absorption and fluorescence measurements. Column chromatography was performed with E. Merck 0.040–0.063 mm Art. 11567 silica gel. ^{1}H NMR, ^{13}C NMR, and ^{31}P NMR were recorded on Bruker AV 300 or AV 400 instruments. All signals were expressed as ppm downfield from Me_4Si for ^{1}H and ^{13}C NMR and from H_3PO_4 for ^{31}P NMR used as an internal standard (δ). Coupling constants (J) are reported in Hz and refer to apparent peak multiplicities. Melting points were measured in open capillary tubes. Mass spectrometry analyses were performed at the Ecole Nationale Supérieure de Chimie de Paris by using a Hewlett–Packard HP 5989 A instrument. Direct introduction experiments were performed by chemical ionization with ammonia. Elemental analyses were performed at the Institut de Chimie des Substances Naturelles and high-resolution mass spectra were done at the University of Paris XI (Orsay).

Diphenyl-[4-trimethylsilylethynyl)phenyl]phosphane oxide: Hydrogen peroxide (30% solution, 1.7 mL) was slowly added to a solution of diphenyl-[4-trimethylsilylethynyl)phenyl]phosphane (2 g, 5.58 mmol) in a mixture of dichloromethane (50 mL) and methanol (50 mL). The resulting mixture was stirred at room temperature for 2 h and was then quenched with aqueous Na_2SO_3 solution and extracted with dichloromethane. The combined organic phases were dried ($MgSO_4$), filtered, and concentrated under reduced pressure to give a white solid (2 g, 96%). M.p. 139°C; ^{1}H NMR (300 MHz, $CHCl_3$): δ = 7.65–7.46 (m, 14H; H_{ar}), 0.25 ppm (s, 9H; CH_3); ^{13}C NMR (75 MHz, $CHCl_3$): 132.7 (C-P), 132.4 (2×C-P), 132.2 (2×CH_{ar}), 132.2 (4×CH_{ar}), 132.0 (2×CH_{ar}), 131.9 (2×CH_{ar}), 128.7 (4×CH_{ar}), 127 (C), 104.0, 97.6 (2×C, C≡C), 0.0 ppm (3×CH_3); ^{31}P NMR (121 MHz, $CDCl_3$): δ = 30.0 ppm; MS (CI, NH_3): m/z: 375 $[M+H]^+$; ES HRMS: m/z: calcd for $C_{46}H_{46}O_2P_2Na$: 771.26; found: 771.24 $[2M+Na]^+$.

Diphenyl-(4-ethynylphenyl)phosphane oxide (2d): Potassium carbonate (256 mg, 1.8 mmol) was added to a solution of diphenyl-[4-(trimethylsilylethynyl)phenyl]phosphane oxide (2 g, 5.34 mmol) in a mixture of dichloromethane (40 mL) and methanol (60 mL). The resulting mixture was stirred at room temperature for 2 h, quenched with water, and then extracted with dichloromethane. The combined organic layers were dried ($MgSO_4$), filtered, and concentrated under reduced pressure to give a white solid (1.4 g, 85%). M.p. 144°C; ^{1}H NMR (300 MHz, $CHCl_3$): δ = 7.69–7.53 (m, 10H; H_{ar}), 7.50–7.43 (m, 4H; H_{ar}), 3.20 ppm (s, 1H; $H_{C\equiv CH}$); ^{13}C NMR (75 MHz, $CHCl_3$): δ = 133.1 (C-P), 132.1 (2×C-P), 132.1 (4×CH_{ar}), 132.0 (2×CH_{ar}), 131.9 (2×CH_{ar}), 128.6 (4×CH_{ar}), 126.9 (2×CH_{ar}), 125.9 (C), 82.6, 79.9 ppm (2×C, C≡C); ^{31}P NMR (121 MHz, $CDCl_3$): δ = 28.7 ppm; MS (CI, NH_3): $C_{20}H_{15}OP$: m/z: 303 $[M+H]^+$; ES HRMS: m/z: calcd for $C_{20}H_{15}OPNa$: 325.0753; found: 325.0765 $[M+Na]^+$.

[4-(10-Bromoanthracen-9-ylethynyl)-phenyl]-dimethyl-amine (10): CuI (26.3 mg, 0.14 mmol) and $Pd(PPh_3)_4$ (159 mg, 0.14 mmol) were added to a solution of 9,10-dibromoanthracene (2.3 g, 6.89 mmol) and 4-ethynyl-*N*,*N*-dimethylbenzylamine (1 g, 6.89 mmol) in a mixture of toluene (70 mL) and triethylamine (20 mL). The resulting mixture was stirred for 24 h at 50°C, and was then allowed to cool to room temperature and concentrated under vacuum. The residue was purified by silica gel chromatography (dichloromethane/cyclohexane 90:10) to give an orange solid (1.3 g, 50%). M.p. 236°C; ^{1}H NMR (300 MHz, $CHCl_3$): δ = 8.73–8.70

(m, 2H; H_{1ar}), 8.57–8.54 (m, 2H; H_{2ar}), 7.66–7.57 (m, 6H; H_{2ar}, H_{3ar}, H_{5ar}), 6.76 (d, J = 9.2 Hz, 2H; H_{6ar}), 3.05 ppm (s, 6H; CH_3); ^{13}C NMR (75 MHz, $CHCl_3$): δ = 150.6 (C), 133.0 (2×CH_{ar}), 132.8 (2×C), 130.5 (2×C), 128.2 (2×CH_{ar}), 127.7 (2×CH_{ar}), 127.5 (2×CH_{ar}), 126.5 (2×CH_{ar}), 122.9 (C), 119.7 (C), 112.1 (2×CH_{ar}), 110.2 (C), 103.8 (C), 84.4 (C), 40.4 ppm (CH_3); MS (CI, NH_3): $C_{24}H_{18}BrN$: m/z: 402 $[M+H]^+$.

Diphenyl-{4-[10-(4-dimethylaminophenylethynyl)anthracen-9-ylethynyl]-phenyl}phosphane oxide (3): CuI (1.91 mg, 0.01 mmol) and $Pd(PPh_3)_4$ (12 mg, 0.01 mmol) were added to a solution of **10** (145 mg, 0.33 mmol) and the phosphane oxide **2d** (100 mg, 0.33 mmol) in a mixture of toluene (15 mL) and triethylamine (4 mL). The resulting mixture was stirred at room temperature for 24 h at 50 °C, and was then allowed to cool to room temperature and concentrated under vacuum. The residue was purified by silica gel chromatography (dichloromethane/acetone 95:5) to give an orange solid (70 mg, 30 %). M.p. > 300 °C; ^{1}H NMR (300 MHz, $CHCl_3$): δ = 8.73–8.61 (m, 4H; H_{1ar}), 7.84–7.50 (m, 6H; H_{ar}), 6.76 (d, J = 8.8 Hz, 2H; H_{ar}), 3.06 ppm (s, 6H; CH_3); ^{13}C NMR (75 MHz, $CHCl_3$): δ = 150.7 (C-N), 133.1 (2×CH_{ar}), 132.6 (C), 132.5 (2×CH_{ar}), 132.4 (2×C), 132.3 (4×CH_{ar}), 132.2 (2×C), 131.9 (2×C), 131.6 (2×CH_{ar}), 128.8 (4×CH_{ar}), 127.8 (2×CH_{ar}), 127.5 (C), 127.2 (2×CH_{ar}), 127.0 (2×CH_{ar}), 126.6 (2×CH_{ar}), 120.8 (C), 116.3 (C), 112.1 (2×CH_{ar}), 110.1 (C), 105.1, 102.0, 89.7, 85.0 (4×C, C≡C), 40.4 ppm (CH_3); ^{31}P NMR (121 MHz, $CDCl_3$): δ = 28.9 ppm; MS (CI, NH_3): $C_{44}H_{32}NOP$: m/z: 622 $[M+H]^+$.

Diphenyl-(4-{4-[(4-dimethylaminophenyl)ethynyl]phenylethynyl}-phenyl)phosphane oxide (2b): Compound **2b** was obtained by the same experimental procedure as used to prepare **3**, starting from a solution of [4-(4-iodophenylethynyl)phenyl]-dimethylamine (**6**, 527 mg, 1.51 mmol) and the phosphane oxide **2d** (100 mg, 0.33 mmol) in a mixture of toluene (18 mL) and triethylamine (4 mL) with CuI (14 mg, 0.07 mmol) and [Pd-$(PPh_3)_4$] (39 mg, 0.03 mmol), to afford a yellow solid (316 mg, 67 %). M.p. 269–271 °C; ^{1}H NMR (300 MHz, $CHCl_3$): δ = 7.70–7.47 (m, 18H; H_{ar}), 7.40 (d, J = 9 Hz, 2H; H_{ar}), 6.66 (d, J = 9 Hz, 2H; H_{ar}), 2.99 ppm (s, 6H; CH_3); ^{13}C NMR (100 MHz, $CHCl_3$): δ = 150.4 (C-N), 132.9 (2×C_{ar}), 132.4 (C-P), 132.3 (2×C-P), 132.2 (4×CH_{ar}), 132.2 (2×CH_{ar}), 132.1 (2×CH_{ar}), 131.7 (2×CH_{ar}), 131.5 (2×CH_{ar}), 131.3 (2×CH_{ar}), 128.7 (4×CH_{ar}), 127.1 (C), 124.8 (C), 121.4 (C), 111.9 (C), 109.6, 93.3, 89.9, 87.3 (4×C, C≡C), 40.3 ppm (2×CH_3); ^{31}P NMR (121 MHz, $CDCl_3$): δ = 30.0 pm; MS (CI, NH_3): $C_{36}H_{28}NOP$: m/z: 522 $[M+H]^+$; elemental analysis calcd (%) for $C_{36}H_{28}NOP$: C 82.90, H 5.41, N 2.69; found: C 82.88, H 5.45, N 2.65.

Tris-(4-{4-[(4-dimethylaminophenyl)ethynyl]phenylethynyl}phenyl)phosphane oxide (1b): Compound **1b** was prepared by the same experimental procedure as used to prepare **3**, starting from a solution of [4-(4-iodophenylethynyl)phenyl]dimethylamine (**6**, 600 mg, 1.75 mmol) and tris-(4-ethynylphenyl)phosphane oxide (**1d**, 121 mg, 0.35 mmol) in a mixture of toluene (20 mL) and triethylamine (4 mL) with CuI (16 mg, 0.07 mmol) and $Pd(PPh_3)_4$ (44 mg, 0.035 mmol), to afford a yellow solid (261 mg, 74 %). M.p. 246–248 °C; ^{1}H NMR (300 MHz, $CHCl_3$): δ = 7.67–7.61 (m, 12H; H_{ar}), 7.50–7.47 (m, 12H; H_{ar}), 7.41 (d, J = 7.2 Hz, 6H; H_{ar}), 6.66 (d, J = 7.2 Hz, 6H; H_{ar}), 3.00 ppm (s, 18H; CH_3); ^{13}C NMR (100 MHz, $CHCl_3$): δ = 150.4 (3×C-N), 132.9 (6×CH_{ar}), 132.1 (6×CH_{ar}), 131.7 (6×CH_{ar}), 131.7 (6C), 131.7 (3×C–P), 131.3 (6×CH_{ar}), 127.5 (3C), 124.9 (3C), 121.4 (3C), 111.9 (6C), 109.7 (3C), 93.3, 92.4, 89.8, 87.3 (4×C, C≡C), 40.3 ppm (6×CH_3); ^{31}P NMR (121 MHz, $CDCl_3$): δ = 28.2 ppm; elemental analysis calcd (%) for $C_{72}H_{54}N_3OP$: C 85.77, H 5.40, N 4.17; found: C 85.69, H 5.66, N 4.16.

Tris-[4-(4-dimethylaminophenylethynyl)phenyl]phosphane oxide (1c): Compound **1c** was obtained by the same experimental procedure as used to prepare **3**, starting from a solution of (4-iodophenyl)-dimethylamine (**9**, 500 mg, 2 mmol) and tris-(4-ethynylphenyl)phosphane oxide (**1d**, 177 mg, 0.5 mmol) in a mixture of toluene (26 mL) and triethylamine (7 mL) with CuI (19 mg, 0.1 mmol) and $[Pd(PPh_3)_4]$ (58 mg, 0.05 mmol), to afford a yellow solid (110 mg, 30 %). M.p. > 300 °C; ^{1}H NMR (300 MHz, $CHCl_3$): δ = 7.60–7.55 (m, 12H; H_{ar}), 7.40 (d, J = 9 Hz, 6H; H_{ar}), 6.65 (d, J = 9 Hz, 6H; H_{ar}), 2.99 ppm (s, 18H; CH_3); ^{13}C NMR (75 MHz, $CHCl_3$): δ = 150.5 (3×C-N), 133.1 (6×CH_{ar}), 132.0 (6×CH_{ar}), 130.8 (3×C-P), 128.4 (3C), 111.9 (6×CH_{ar}), 109.3 (3C), 94.1, 86.9 (2×C, C≡C), 40.3 ppm (6×CH_3); ^{31}P NMR (121 MHz, $CDCl_3$): δ = 28.7; MS (CI, NH_3): $C_{48}H_{42}N_3OP$: m/z: 709 $[M+H]^+$.

Theoretical methods: The all-valence INDO (intermediate neglect of differential overlap) method[23] was employed for the calculation of the electronic spectra of the six molecules. The monoexcited configuration interaction (MECI) approximation was employed to describe the excited states. The 100 lowest-energy one-electron transitions between the 10 highest occupied molecular orbitals and the 10 lowest unoccupied ones were chosen to undergo CI mixing. Calculations were performed with the aid of the commercially available MSI software package ZINDO.[24] In the absence of molecular structures, metrical parameters used for the INDO calculations were obtained from gas-phase geometry optimization performed at the PM3 level (MOPAC) in the Gaussian98 package.[25] The starting fragments used to build the molecules were taken from previously reported related crystal structures.[26] Molecules **1a**, **1b**, and **1c** were found to possess roughly C_3 symmetry axes, within ranges of uncertainty of 0.20, 0.35, and 0.15 Å, respectively, so strict C_3 symmetries were imposed for these three molecules in the final optimization processes. The calculated structures have been included as Supporting Information.

Spectroscopic measurements: UV/Vis absorption spectra were recorded on a Varian Cary5E spectrophotometer and corrected emission spectra were obtained on a Jobin–Yvon Spex Fluorolog 1681 spectrofluorimeter. The fluorescence quantum yields were determined by using quinine sulfate dihydrate in sulfuric acid (0.5 N; Φ_F = 0.546[27]) or coumarin C153 in ethanol (Φ_F = 0.38[28]) as standards. For the emission measurements, the absorbances at the excitation wavelengths were below 0.1 and so the concentrations were below 10^{-5} mol L^{-1}.

The oscillator strength of a transition is given by the following equation:

$$f = 4.315 \times 10^{-9} \varepsilon \Delta E^{[29]}$$

Fluorescence intensity decays were obtained by the single-photon timing method with picosecond laser excitation by use of a Spectra-Physics set-up composed of a titanium sapphire Tsunami laser pumped by an argon ion laser, a pulse detector, and doubling (LBO) and tripling (BBO) crystals. Light pulses were selected by optoaccoustic crystals at a repetition rate of 4 MHz. Fluorescence photons were detected through a long-pass filter (375 nm) by means of a Hamamatsu MCP R3809U photomultiplier, connected to a constant-fraction discriminator. The time-to-amplitude converter was purchased from Tennelec. Data were analyzed by a nonlinear least-squares method with the aid of Globals software (Globals Unlimited, University of Illinois at Urbana-Champaign, Laboratory of Fluorescence Dynamics).

EFISHG measurements: Measurements were performed at 1907 nm. This wavelength was generated by focusing the 1064 nm fundamental beam of a nanosecond Nd:YAG pulsed laser in a Raman-shifting hydrogen cell (40 bar, 1 m long) and used as the fundamental beam for SHG measurements. The SHG intensity was detected by use of a photomultiplier (Hamamatsu) and the signal was read on an oscillator (Tektronic TDS 620). The centrosymmetry of the solution was broken by application of a pulsed electric field of 5 kV for 5 μs (Lasermetrics). A solution of MNA (2-methyl-4-nitroaniline, $\mu\beta$ = 71×10^{-48} esu at 1907 nm)[30] served as reference. These measurements were performed for each molecule with increasing concentrations in chloroform. Detailed set-up and data analysis method have been described elsewhere.[31]

Ground-state dipole moments: Dielectric constants and refractive indexes of solutions of increasing concentration were measured on an HP 4192 A impedance analyzer and an Abbe refractometer (Carl Zeiss), respectively. From these data, Guggenheim's method was used to determine the ground state dipole moments.[32]

Acknowledgements

This work was supported by the French Research Ministry program "ACI Jeune Chercheur 2004–2006". We are grateful to J.-P. Lefevre and J.-J. Vachon for their assistance in tuning the single-photon timing instruments. The authors acknowledge B. Valeur for fruitful discussions. M.-H.

Ha-Thi is grateful to the Ministère de l'Education et de la Recherche for a grant (2004–2007).

[1] a) Nonlinear Optical Properties of Organic Molecules and Crystals *, Vol. 1, 2* (Eds.: D. S. Chemla, J. Zyss), Academic Press, New York, **1987**; b) *Molecular Nonlinear Optics: Materials, Phenomena and Devices* (Ed.: J. Zyss), *Chem. Phys.* **1999**, 245 (special issue); c) *C.R. Acad. Sc. Phys.* **2002**, *3*, 403–559 (special issue).

[2] B. Valeur, *Molecular Fluorescence. Principles and Applications*, Wiley-VCH, Weinheim, **2002**.

[3] a) A. P. de Silva, H. Q. N. Gunaratne, T. Gunnlaugsson, A. J. M. Huxley, C. P. McCoy, J. T. Rademacher, T. E. Rice, *Chem. Rev.* **1997**, *97*, 1515–1566; b) *Chemosensors of Ion and Molecule Recognition* (Eds.: J. P. Desvergne, A. W. Czarnik), Kluwer Academic Publishers, Dordrecht, **1997**; c) B. Valeur, I. Leray, *Coord. Chem. Rev.* **2000**, *205*, 3–40; d) J. D. Winkler, C. M. Bowen, V. Michelet, *J. Am. Chem. Soc.* **1998**, *120*, 3237–3242; e) G. E. Collins, L. S. Choi, K. J. Ewing, V. Michelet, C. M. Bowen, J. D. Winkler, *Chem. Commun.* **1999**, *4*, 321–322.

[4] a) I. Leray, J. P. Lefèvre, J.-F. Delouis, J. Delaire, B. Valeur, *Chem. Eur. J.* **2001**, *7*, 4590–4598; b) R. Métivier, I. Leray, B. Valeur, *Chem. Commun.* **2003**, 996–997; c) R. Métivier, I. Leray, B. Valeur, *Chem. Eur. J.* **2004**, *10*, 4480–4490.

[5] a) U. H. F. Bunz, *Chem. Rev.* **2000**, *100*, 1605–1644; b) O. Mongin, L. Porrès, L. Moreaux, J. Mertz, M. Blanchard-Desce, *Org. Lett.* **2002**, *4*, 719–722; c) M. Biswas, P. Nguyen, T. B. Marder, L. R. Khundkar, *J. Phys. Chem. A* **1997**, *101*, 1689–1695.

[6] a) A. Amini, A. Harriman, *Phys. Chem. Chem. Phys.* **2003**, *5*, 1344–1351; b) A. Elangovan, K.-M. Kao, S.-W. Yang, Y.-L. Chen, T.-I. Ho, Y. O. Su, *J. Org. Chem.* **2005**, *70*, 4460–4469; c) S.-W. Yang, A. Elangovan, K.-C. Hwang, T.-I. Ho, *J. Phys. Chem. B* **2005**, *109*, 16628–16635; d) D. P. Lydon, L. Porrès, A. Beeby, T. B. Marder, P. J. Low, *New J. Chem.* **2005**, *29*, 972–976; e) J.-H. Lin, A. Elangovan, T.-I. Ho, *J. Org. Chem.* **2005**, *70*, 7397–7407; f) R. Ponce Ortiz, R. Malavé Osuna, M. C. Delgado, J. Casado, S. A. Jenekhe, V. Hernandez, J. T. Lopez Navarete, *Int. J. Quantum Chem.* **2005**, *104*, 635–644; g) R. C. Smith, M. J. Earl, J. D. Protasiewicz, *Inorg. Chim. Acta* **2004**, *357*, 4139–4143; h) A. Elangovan, S.-W. Yang, J.-H. Lin, K.-M. Kao, T.-I. Ho, *Org. Biomol. Chem.* **2004**, *2*, 1597–1602.

[7] a) K. Kondo, T. Fujitani, N. Ohnishi, *J. Mater. Chem.* **1997**, *7*, 429–433; b) A. E. Stiegman, E. Graham, K. J. Perry, L. R. Khundkar, L.-T. Cheng, J. W. Perry, *J. Am. Chem. Soc.* **1991**, *113*, 7658–7666; c) J. J. Wolff, R. Wortmann, *Adv. Phys. Org. Chem.* **1999**, *32*, 121.

[8] R. Métivier, R. Amengual, I. Leray, V. Michelet, J.-P. Genêt, *Org. Lett.* **2004**, *6*, 739–742.

[9] W. J. Yang, C. H. Kim, M. Y. Jeong, S. K. Lee, M. Y. Piao, S. J. Jeon, B. R. Cho, *Chem. Mater.* **2004**, *16*, 2783–2789.

[10] a) O. O. Orazi, R. A. Corral, H. E. Bertorello, *J. Org. Chem.* **1965**, *30*, 1101–1104; b) H. Gilman, L. Summers, *J. Am. Chem. Soc.* **1950**, *72*, 2767–2768; c) A. G. Giumanini, G. Chiavari, M. M. Musiani, P. Rossi, *Synthesis* **1980**, 743–746.

[11] H. Meier, B. Mühling, H. Kolshorn, *Eur. J. Org. Chem.* **2004**, 1033–1042.

[12] a) Y. Yamagushi, T. Tanaka, S. Kobayashi, T. Wakamiya, Y. Matsubara, Z. Yoshiba, *J. Am. Chem. Soc.* **2005**, *127*, 9332–9333; b) Y. Yamagushi, S. Kobayashi, T. Wakamiya, Y. Matsubara, Z.-I. Yoshida, *Angew. Chem.* **2005**, *117*, 7202–7206; *Angew. Chem. Int. Ed.* **2005**, *44*, 7040–7044.

[13] C. Katan, F. Terenziani, O. Mongin, M. H. Wertz, L. Porres, T. Pons, J. Mertz, S. Tretiak, M. Blanchard-Desce, *J. Phys. Chem. A* **2005**, *109*, 3024–3037.

[14] a) N. Mataga, Y. Kaifu, M. Koizumi, *Bull. Chem. Soc. Jpn.* **1955**, *28*, 690–691; b) E. Z. Lippert, *Z. Naturforsch. A* **1955**, *10*, 541–545.

[15] P. Suppan, *J. Photochem. Photobiol. A* **1990**, *50*, 293–330.

[16] S. Di Bella, T. J. Marks, M. A. Ratner, *J. Am. Chem. Soc.* **1994**, *116*, 4440–4445.

[17] Y. Hirata, T. Okada, T. Nomoto, *J. Phys. Chem.* **1998**, *102*, 6585–6589.

[18] J. J. Wolff, F. Siegler, R. Matschiner, R. Wortmann, *Angew. Chem.* **2000**, *112*, 1494–1498; *Angew. Chem. Int. Ed.* **2000**, *39*, 1436–1439.

[19] a) J. L. Oudar, *J. Chem. Phys.* **1977**, *67*, 446–457; b) J. L. Oudar, D. S. Chemla, *J. Chem. Phys.* **1977**, *66*, 2664–2668.

[20] D. J. Williams, *Angew. Chem.* **1984**, *96*, 637–651; *Angew. Chem. Int. Ed. Engl.* **1984**, *23*, 690–703.

[21] D. R. Kanis, M. A. Ratner, T. Marks, *Chem. Rev.* **1994**, *94*, 195–242.

[22] J. Zyss, J. L. Oudar, *Phys. Rev. A* **1982**, *26*, 2028–2048.

[23] a) M. Zerner, G. Loew, R. Kirchner, U. Mueller-Westerhoff, *J. Am. Chem. Soc.* **1980**, *102*, 589–599; b) W. P. Anderson, D. Edwards, M. C. Zerner, *Inorg. Chem.* **1986**, *25*, 2728–2732.

[24] ZINDO, release 96.0, Molecular Simulations Inc.: Cambridge (UK), **1996**.

[25] Gaussian 98, Revision A.7, M. J. Frisch, G. W. Trucks, H. B. Schlegel, G. E. Scuseria, M. A. Robb, J. R. Cheeseman, V. G. Zakrzewski, J. A. Montgomery, Jr., R. E. Stratmann, J. C. Burant, S. Dapprich, J. M. Millam, A. D. Daniels, K. N. Kudin, M. C. Strain, O. Farkas, J. Tomasi, V. Barone, M. Cossi, R. Cammi, B. Mennucci, C. Pomelli, C. Adamo, S. Clifford, J. Ochterski, G. A. Petersson, P. Y. Ayala, Q. Cui, K. Morokuma, D. K. Malick, A. D. Rabuck, K. Raghavachari, J. B. Foresman, J. Cioslowski, J. V. Ortiz, A. G. Baboul, B. B. Stefanov, G. Liu, A. Liashenko, P. Piskorz, I. Komaromi, R. Gomperts, R. L. Martin, D. J. Fox, T. Keith, M. A. Al-Laham, C. Y. Peng, A. Nanayakkara, C. Gonzalez, M. Challacombe, P. M. W. Gill, B. Johnson, W. Chen, M. W. Wong, J. L. Andres, C. Gonzalez, M. Head-Gordon, E. S. Replogle, J. A. Pople, Gaussian, Inc., Pittsburgh PA, **1998**.

[26] a) M. R. Churchill, R. F. See, S. L. Randall, J. D. Atwood, *Acta Crystallogr. Sect. C Cryst. Struct. Commun.* **1993**, *49*, 345–347; b) E. M. Graham, V. M. Miskowski, J. W. Perry, D. R. Coulter, A. E. Stiegman, W. P. Schaefer, R. E. Marsh, *J. Am. Chem. Soc.* **1989**, *111*, 8771–8779; c) M. Lequan, R. M. Lequan, K. Chane-Ching, P. Bassoul, G. Bravic, Y. Barrans, D. Chasseau, *J. Mater. Chem.* **1996**, *6*, 5–9.

[27] J. N. Demas, G. A. Crosby, *J. Phys. Chem.* **1971**, *75*, 991–1024.

[28] G. A. Reynolds, K. H. Drexhage, *Opt. Commun.* **1975**, *13*, 222–225.

[29] M. Orchin, H. H. Jaffé, *Symmetry Orbitals, and Spectra*, Wiley, New York, **1971**, p. 204.

[30] a) C. Bosshard, G. Knöpfle, P. Prêtre, P. Günter, *J. Appl. Phys.* **1992**, *71*, 1594–1605.

[31] a) I. Maltey, J. A. Delaire, K. Nakatani, P. Wang, X. Shi, S. Wu, *Adv. Mater. Opt. Electron.* **1996**, *6*, 233–238; b) C. S. Liu, R. Glaser, P. Sharp, J. F. Kauffmann, *J. Phys. Chem. A* **1997**, *101*, 7176–7181.

[32] E. A. Guggenheim, *Trans. Faraday Soc.* **1949**, *45*, 714–720.

Received: April 3, 2006
Revised: June 13, 2006
Published online: September 6, 2006

